Structure of the doublet bands in doubly odd nuclei: The case of ^{128}Cs

H. G. Ganev[1] and S. Brant[2]

[1]*Institute of Nuclear Research and Nuclear Energy, Bulgarian Academy of Sciences, Sofia 1784, Bulgaria*
[2]*Department of Physics, Faculty of Science, University of Zagreb, 10000 Zagreb, Croatia*

The structure of the $\Delta J = 1$ doublet bands in ^{128}Cs is investigated within the framework of the interacting vector boson-fermion model. A new, purely collective interpretation of these bands is given on the basis of the used boson-fermion dynamical symmetry of the model. The energy levels of the doublet bands as well as the absolute $B(E2)$ and $B(M1)$ transition probabilities between the states of both yrast and yrare bands are described quite well. The observed odd-even staggering of both $B(M1)$ and $B(E2)$ values is reproduced by the introduction of an appropriate interaction term of quadrupole type, which produces such a staggering effect in the transition strengths. The calculations show that the appearance of doublet bands in certain odd-odd nuclei could be a consequence of the realization of a larger dynamical symmetry based on the noncompact supersymmetry group OSp$(2\Omega/12, \text{R})$.

I. INTRODUCTION

One of the most intriguing phenomena that has attracted significant attention and intensive discussion in the last decade is the appearance of the nearly degenerate $\Delta J = 1$ doublet bands with the same spins and parities in odd-odd $N = 75$ and $N = 73$ isotones in the $A \sim 130$ region. A large number of experimental data [1–8] have been accumulated in this mass region which showed that the yrast and yrare states are built on the $\pi h_{11/2} \otimes \nu h_{11/2}$ configuration. Pairs of bands have been found also in the $A \sim 105$ and $A \sim 190$ mass regions. Initially, these $\Delta J = 1$ doublet bands were interpreted as a manifestation of "chirality" in the sense of the angular momentum coupling [9]. Several theoretical models have been applied in a number of articles, like the tilted axis cranking model [1,2,8,10], the core-quasiparticle coupling model (CQPCM) [11], the particle-rotor model [4,5,12], the two quasiparticle + triaxial rotor model [13], and the core-particle-hole coupling model [7]. All these models have one assumption in common: they suppose a rigid triaxial core and hence support the interpretation of the doublet bands of chiral structure. On the contrary, all odd-odd nuclei in which twin bands have been observed have a different characteristic in common: they are in regions where even-even nuclei are γ soft. Their potential energy surface is rather flat in the γ direction and the couplings with other core structures, not only the ground state band, are significant. Nevertheless, it was shown in [14] that the odd-odd nuclei with soft cores have chiral properties similar to those with rigid core structures. Although the odd-odd nuclei in the $A \sim 130$ region should properly be described by soft cores, the rigidity does not seem to be decisive for chirality [7].

Many of the recent experiments and theoretical analyses do not support completely the chiral interpretation [15–18]. In particular, in an ideal situation, that is, orthogonal angular momentum vectors and stable triaxial nuclear shape, states with the same spin should be observed close in excitation energy. In fact, the attainment of such near-degeneracy is one of the key characteristics of chirality. This feature has

not been observed in any of the chiral structures identified to date. Moreover, states with different structure in two nonchiral bands can also accidentally be close in excitation energy. Thus, one of the important tests of chirality is that the partner states in the two bands should also have similar physical properties, such as moment of inertia, quasiparticle alignments, transition quadrupole moments, and the related $B(E2)$ values for intraband $E2$ transitions. Some experimental studies have shown that the two bands have different shapes due to the different kinematical moments of inertia, which suggest a shape coexistence (triaxial and axial shapes). This is an interesting observation since the quantal nature of chirality automatically demands that a chiral partner band should have identical properties to the yrast triaxial rotational band. Similarly, it was also found for some of the proposed chiral nuclei that the experimental data for the behavior of other observables [equal $E2$ transitions increasing with spin, staggering behavior of the $M1$ values, the smoothness of the signature $S(J)$, etc.] do not support such a chiral structure [15–18]. These results demand a deeper and more detailed discussion of our understanding of the origin of doublet bands. Although the odd-odd nuclei in the considered mass region do not satisfy all the requirements for the existence of chirality, they can approach some of them, or at least retain some fingerprints of chirality. In this respect it is appropriate to consider the observation of nearly degenerate doublet bands exhibiting some of the chiral features as manifestation of the (weak) chiral symmetry breaking phenomenon [6,19].

The fact that two bands of the same parity have levels of the same spin close in excitation energy is not a very strong argument to claim that they are chiral bands. In order to establish their chiral structure it is crucial to determine the $B(E2)$ and $B(M1)$ values. In this respect, lifetime measurements are essential for extracting the absolute $B(E2)$ and $B(M1)$ transition probabilities, which are critical experimental observables in addition to the energy levels. In a number of papers (e.g., [20]) the observation of $B(M1)$ staggering was suggested as the main fingerprint for the identification of the chiral doublet bands. Strong staggering

is considered as manifestation of static chirality, whereas weak staggering was interpreted as a chiral vibration [21]. Characteristic properties of the chiral bands are closely connected with the triaxiality (rigid or soft) and the deviation from maximal triaxiality causes fast splitting of the partner bands [14] and the vanishing of the $B(M1)$ [and $B(E2)$] staggering [22].

Within the framework of the pair truncated shell model (PTSM), it was pointed out that the band structure of the doublet bands can be explained by the chopstickslike motion of two angular momenta of the odd neutron and the odd proton [23]. It was found that the level scheme of $\Delta J = 1$ doublet bands does not arise from the chiral structure, but from different angular momentum configurations of the unpaired neutron and unpaired proton in the $0h_{11/2}$ orbitals, weakly coupled with the collective excitations of the even-even core. The same interpretation was given also in the quadrupole coupling model (QCM) [24,25].

An alternative interpretation is based on the interacting boson-fermion-fermion model (IBFFM) [26], where the energy degeneracy is obtained but a different nature is attributed to the two bands. A detailed analysis of the wave functions in the IBFFM showed as well that the presence of configurations with the angular momenta of the proton, neutron, and core in the chirality-favorable, almost orthogonal geometry, is substantial but far from being dominant. The large fluctuations of the deformation parameters β and γ around the triaxial equilibrium shape enhance the content of achiral configurations in the wave functions. The composition of the yrast band, in terms of contributions from core states, shows that the yrast band is basically built on the ground-state band of the even-even core. With increasing spin the admixture of the γ band of the core becomes more pronounced. The sideband wave functions contain large components of the γ band and, with increasing spin, of higher-lying collective structures of the core, which near the band crossing become dominant. Thus, according to the IBFFM the existence of twin bands should be attributed to a weak dynamic (fluctuation-dominated) chirality.

The above variety of models and approaches dealing with the description of the doublet bands in odd-odd nuclei reveals the complexity of the chiral rotation and motivated us to consider their properties in the framework of the boson-fermion extension [27] of the symplectic interacting vector boson model (IVBM), for which we will use the term interacting vector boson-fermion model (IVBFM). In [28] the investigation of the doublet bands in some doubly odd nuclei from the $A \sim 130$ region was presented. A good agreement between experiment and theoretical predictions for the energy levels of these bands as well as in-band $B(E2)$ and $B(M1)$ transition probabilities is obtained. With the present work, we exploit further the new dynamical symmetry [27,28] of the IVBFM for the analysis of the structure of the $\pi h_{11/2} \otimes \nu h_{11/2}$ positive-parity doublet bands in ^{128}Cs. Recently, lifetime measurements in ^{128}Cs were performed to extract the absolute transition probabilities $B(M1)$ and $B(E2)$ to identify candidate chiral doublet bands [29]. The partner bands in ^{128}Cs with similar $B(M1)$ and $B(E2)$ transitions and strong $B(M1)$ staggering were observed and regarded

as the best known example revealing the chiral symmetry breaking phenomenon [6,19]. A systematic study of doublet bands in the nearby odd-odd ^{128}Cs–^{134}Cs isotopes was done in [6]. In an attempt to search for the chiral doublet bands in ^{126}Cs, high-spin states of ^{126}Cs were investigated in [30] and candidate chiral doublet bands in ^{126}Cs were proposed. Based on a systematic comparison with the neighboring odd-odd Cs isotopes, a pair of chiral doublet bands in ^{122}Cs are proposed in [31].

The spectrum of the positive-parity states in ^{128}Cs considered in this paper is based on the odd proton and odd neutron that occupy the same single-particle level $h_{11/2}$. The theoretical description of the doubly odd nuclei under consideration is fully consistent and starts with the calculation of their even-even and odd-even neighbors. We consider the simplest physical picture in which two particles occupying the same single-particle level j are coupled to an even-even core nucleus whose states belong to an Sp(12, R) irreducible representation. Within the framework of the IVBFM a purely collective structure of the doublet bands is obtained. To describe the structure of odd-odd nuclei, first a description of the appropriate even-even cores should be obtained.

II. THE EVEN-EVEN CORE NUCLEUS

The algebraic structure of the IVBM is realized in terms of creation and annihilation operators of two kinds of vector bosons $u_m^\dagger(\alpha), u_m(\alpha)$ ($m = 0, \pm1$), which differ in an additional quantum number $\alpha = \pm1/2$—the projection of the T spin (an analog to the F spin of Interacting Boson Model-2). One might consider these two bosons just as building blocks or "quarks" of elementary excitations (phonons) rather than real fermion pairs, which generate a given type of symmetry. In this regard, the s and d bosons of the IBM can be considered as bound states of elementary excitations generated by two vector bosons. Thus, we assume that it is the type of symmetry generated by the bosons that is of importance for the description of the collective motions in nuclei.

All bilinear combinations of the creation and annihilation operators of the two vector bosons generate the boson representations of the noncompact symplectic group Sp^B(12, R) [32]:

$$F_M^L(\alpha, \beta) = \sum_{k,m} C_{1k1m}^{LM} u_k^\dagger(\alpha) u_m^\dagger(\beta), \tag{1}$$

$$G_M^L(\alpha, \beta) = \sum_{k,m} C_{1k1m}^{LM} u_k(\alpha) u_m(\beta), \tag{2}$$

$$A_M^L(\alpha, \beta) = \sum_{k,m} C_{1k1m}^{LM} u_k^+(\alpha) u_m(\beta), \tag{3}$$

where C_{1k1m}^{LM}, which are the usual Clebsch-Gordan coefficients for $L = 0, 1, 2$ and $M = -L, -L+1, \ldots, L$, define the transformation properties of (1), (2) and (3) under rotations. Being a noncompact group, the unitary representations of Sp^B(12, R) are of infinite dimension, which makes it impossible to diagonalize the most general Hamiltonian. When reduced to the group U^B(6), each irreducible representation (irrep) of the group Sp^B(12, R) decomposes into irreps of the subgroup characterized by the partitions [32] $[N, 0^5]_6 \equiv [N]_6$,

where $N = 0, 2, 4, \ldots$ (even irrep) or $N = 1, 3, 5, \ldots$ (odd irrep). The subspaces $[N]_6$ are finite dimensional, which simplifies the problem of diagonalization. Therefore the complete spectrum of the system can be calculated through the diagonalization of the Hamiltonian in the subspaces of all the unitary irreducible representations (UIRs) of $U^B(6)$, belonging to a given UIR of $Sp^B(12, R)$, which further clarifies its role as a group of dynamical symmetry.

The most important application of the $U^B(6) \subset Sp^B(12, R)$ limit of the theory is the possibility it affords of describing both even and odd parity bands up to very high angular momentum [32]. In order to do this we first have to identify the experimentally observed bands with the sequences of basis states of the even $Sp^B(12, R)$ irrep (Table I). Since we deal with the symplectic extension, we are able to consider all even eigenvalues of the number of vector bosons N with the corresponding set of T spins, which uniquely define the $SU^B(3)$ irreps (λ, μ). The multiplicity index K appearing in the final reduction to the $SO^B(3)$ is related to the projection of L on the body-fixed frame and is used with the parity (π) to label the different bands (K^π) in the energy spectra of the nuclei. For the even-even nuclei we have defined the parity of the states as $\pi_{\text{core}} = (-1)^T$ [32]. This allowed us to describe both positive and negative bands.

Further, we use the algebraic concept of "yrast" states, introduced in [32]. According to this concept we consider as yrast states the states with given L that minimize the energy with respect to the number of vector bosons N that build them. Thus the states of the ground-state band (GSB) were identified with the $SU^B(3)$ multiplets $(0, \mu)$ [32]. In terms of (N, T) this choice corresponds to $(N = 2\mu, T = 0)$ and the sequence of states with different numbers of bosons $N = 0, 4, 8, \ldots$ and $T = 0$ (and also $T_0 = 0$). The presented mapping of the experimental states onto the $SU^B(3)$ basis states, using the algebraic notion of yrast states, is a particular case of the so-called stretched states [33]. The latter are defined as the states with $(\lambda_0 + 2k, \mu_0)$ or $(\lambda_0, \mu_0 + k)$, where $N_i = \lambda_0 + 2\mu_0$ and $k = 0, 1, 2, 3, \ldots$. In the symplectic extension of the IVBM the change of the number k, which is related in the applications to the angular momentum L of the states, gives rise to the collective bands.

It was established [34] that the correct placement of the bands in the spectrum strongly depends on their bandheads' configuration, and in particular on the minimal or initial number of bosons, $N = N_i$, from which they are built. The latter determines the starting position of each excited band. In the present application we take for N_i the value at which the best χ^2 is obtained in the fitting procedure for the energies of the excited band considered.

The used Hamiltonian for the core nucleus is [32]

$$H_B = aN + bN^2 + \alpha_3 T^2 + \beta_3 L^2 + \alpha_1 T_0^2, \quad (4)$$

which is expressed in terms of the first- and second-order Casimir operators from the unitary limit [32] of the model [see the boson part of chain (12)]. Taking into account the relations $N = \lambda + 2\mu$ and $T = 2\lambda$ between the quantum numbers of the mutually complementary groups $SU^B(3)$ and $U^B(2)$ in (12), it becomes obvious that H_{core} is diagonal in the
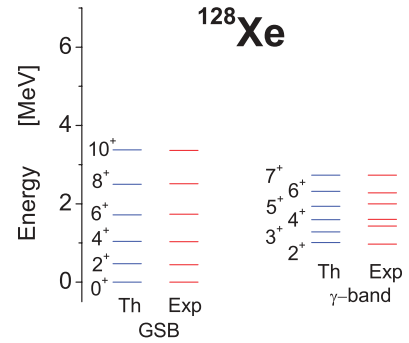

FIG. 1. (Color online) Comparison of the theoretical and experimental energies for the ground and γ bands of ^{128}Xe. The values obtained for the model parameters entering in the core Hamiltonian (4) are $a = 0.089\,09$, $b = -0.004\,59$, $\alpha_3 = 0.024\,71$, $\beta_3 = 0.031\,23$, and $\alpha_1 = -0.019\,89$.

basis

$$|[N]_6; (\lambda, \mu); KLM; T_0\rangle \equiv |(N, T); KLM; T_0\rangle, \quad (5)$$

labeled by the quantum numbers of the subgroups of the chain (12). Its eigenvalues are the energies of the basis states of the boson representations of $Sp(12, R)$:

$$E((N, T), L, T_0) = aN + bN^2 + \alpha_3 T(T + 1) \\ + \beta_3 L(L + 1) + \alpha_1 T_0^2. \quad (6)$$

We determine the values of the five phenomenological model parameters $a, b, \alpha_3, \beta_3, \alpha_1$ by fitting the energies of the ground and γ bands in the ^{128}Xe nucleus to the experimental data [35], using a χ^2 procedure. The theoretical predictions are presented in Fig. 1. From the figure one can see that the calculated energy levels of both ground state and γ bands agree rather well with the observed data.

Numerous IBM studies of even-even nuclei in the $A \sim 130$ mass region have shown that these nuclei are well described by the O(6) symmetry of the IBM, which in the classical limit corresponds to the Wilets-Jean model of a γ-unstable rotor [36], and that the accepted interpretation is that they are γ soft. The core nucleus ^{128}Xe has $R_{4/2} = 2.33$, which is between the U(5) and O(6) values $R_{4/2} = 2.00$ and 2.5, respectively, which reveals the transitional character of this γ-soft nucleus. The value $R_{4/2} = 2.33$ is close to the critical point value $R_{4/2} = 2.20$ for E(5) symmetry, which has served as a ground for some authors to consider ^{128}Xe as an E(5) nucleus. In [37], the predictions of the Z(4) model are compared to existing experimental data for some nuclei, including ^{128}Xe. The reasonable agreement observed in [37] is in no contradiction with the characterization of these nuclei as O(6) nuclei, since it is known [38] that γ-unstable models [like O(6)] and γ-rigid models [like Z(4)] yield similar predictions for most observables if γ_{rms} of the former equals γ_{rigid} of the latter. In [39] a γ-independent version of the confined β-soft (CBS) rotor model, in which the structure of ^{128}Xe was investigated, has been formulated. That version, called O(5) CBS, generalizes the E(5) solution near the critical point to a parametric solution for the whole path between E(5) and the β-rigidly-deformed γ-independent limit. The usage of all these models reveals the transitional character of the ^{128}Xe core
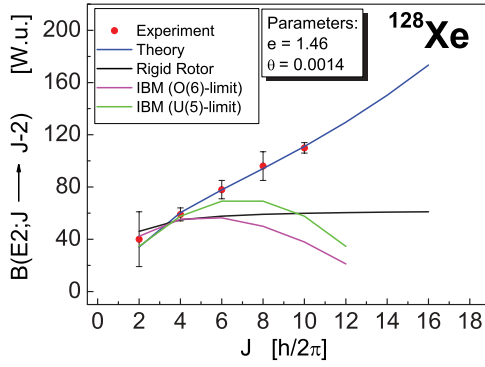
FIG. 2. (Color online) Comparison of the theoretical and experimental values for the $B(E2)$ transition probabilities between the states of the GSB in ^{128}Xe. The theoretical predictions of the rigid rotor and IBM are shown as well. The values of the model parameters are $e = 1.46$ and $\theta = 0.0014$.

nucleus. The transitional properties of the latter can be clearly seen from its electromagnetic properties. Indeed, one can see the characteristic (almost "linear") $B(E2)$ behavior for the ground-state band of ^{128}Xe in Fig. 2, where for comparison the theoretical predictions of the rigid rotor and IBM in its O(6) and U(5) limits are also shown. This behavior differs from the typical paraboliclike (cutoff effect) SU(3), U(5), and O(6) curves. The experimental data are taken from [40]. The value obtained for the quadrupole moment of the 2_1^+ state of GSB is $Q(2) = -0.15$ eb. At this point we want to point out that, because of the mixing of different collective modes within the framework of the symplectic IVBM [32], we are able to describe even-even cores with various collective properties that need different dynamical symmetries or their mixture in the IBM and other algebraic approaches.

III. ORTHOSYMPLECTIC EXTENSION

In order to incorporate the intrinsic spin degrees of freedom into the symplectic IVBM, we extend the dynamical algebra of $Sp^B(12, R)$ to the orthosymplectic algebra of $OSp(2\Omega/12, R)$ [27]. For this purpose we introduce a particle with spin j half integer ($\Omega = 2j + 1$) and consider a simple core-plus-particle picture. Thus, in addition to the boson collective degrees of freedom we introduce creation and annihilation operators $a_m^\dagger$ and a_m ($m = -j, \ldots, j$), which satisfy the anticommutation relations $\{a_m, a_{m'}^\dagger\} = \delta_{mm'}$ and $\{a_m^\dagger, a_{m'}^\dagger\} = \{a_m, a_{m'}\} = 0$.

All bilinear combinations of $a_m^\dagger$ and $a_{m'}$, namely,

$$f_{mm'} = a_m^\dagger a_{m'}^\dagger, \quad m \neq m', \tag{7}$$

$$g_{mm'} = a_m a_{m'}, \quad m \neq m', \tag{8}$$

$$C_{mm'} = (a_m^\dagger a_{m'} - a_{m'} a_m^\dagger)/2, \tag{9}$$

generate the fermion-pair Lie algebra of $SO^F(2\Omega)$. Their commutation relations are given in [27]. The number-preserving operators (9) generate the maximal compact subalgebra of $SO^F(2\Omega)$, that is, $U^F(\Omega)$.

A. Fermion dynamical symmetries

One can further construct a certain fermion dynamical symmetry, that is, the group-subgroup chain:

$$SO^F(2\Omega) \supset G' \supset G'' \supset \cdots. \tag{10}$$

In particular, for one particle occupying a single level j we are interested in the following dynamical symmetry:

$$SO^F(2\Omega) \supset Sp(2j + 1) \supset SU^F(2), \tag{11}$$

where $Sp(2j + 1)$ is the compact symplectic group. The dynamical symmetry (11) remains valid also for the case of two particles occupying the same level j. In this case, the allowed values of the quantum number I of $SU^F(2)$ in (11) according to reduction rules are $I = 0, 2, \ldots, 2j - 1$ [41]. For simplicity hereafter we will use just the reduction $SO^F(2\Omega) \supset SU^F(2)$ and keep in mind the proper content of the set of I values for the one- and/or two-particle cases, respectively. For the $A \sim 130$ region where the doublet bands are built on the $\pi h_{11/2} \otimes \nu h_{11/2}$ configuration, the two fermions occupy the same single-particle level $j_1 = j_2 = j = 11/2$ with negative parity ($\pi_{sp} = -$) and the fermion reduction chain (11) can be used.

B. Dynamical Bose-Fermi symmetry. Dynamical supersymmetry

Once the fermion dynamical symmetry is determined we proceed with the construction of the Bose-Fermi symmetries. If a fermion is coupled to a boson system having itself a dynamical symmetry (e.g., such as an IBM core), the full symmetry of the combined system is $G^B \otimes G^F$. Bose-Fermi symmetries occur if at some point the same group appears in both chains $G^B \otimes G^F \supset G^{BF}$, that is, the two subgroup chains merge into one.

The standard approach to supersymmetry in nuclei (dynamical supersymmetry) is to embed the Bose-Fermi subgroup chain of $G^B \otimes G^F$ into a larger supergroup G, that is, $G \supset G^B \otimes G^F$. Making use of the embedding $SU^F(2) \subset SO^F(2\Omega)$ we use the orthosymplectic (supersymmetric) extension of the IVBM which is defined through the chain [27]

$$
\begin{array}{ccc}
OSp(2\Omega/12, R) \supset SO^F(2\Omega) & \otimes & Sp^B(12, R) \\
& & \cup \\
\cup & \otimes & U^B(6) \\
& & N \\
& & \cup \\
SU^F(2) & \otimes & SU^B(3) \otimes U_T^B(2) \\
I & & (\lambda, \mu) \Longleftrightarrow (N, T) \\
\searrow & & \cup \\
& \otimes & SO^B(3) \otimes SO_T^B(2) \\
& & L \quad\quad T_0 \\
\cup & & \\
Spin^{BF}(3) & \supset & Spin^{BF}(2), \\
J & & J_0
\end{array} \tag{12}
$$

where below the different subgroups the quantum numbers characterizing their irreducible representations are given. $Spin^{BF}(n)$ ($n = 2, 3$) denotes the universal covering group of $SO(n)$.

At this point we want to stress that, although the "coupling" of a particle (or two-particle system) to the symplectic core is done at the SU(2) level, the present situation is not identical to that of the IBFM. In fact, in our approach because of the (ortho)symplectic structures [allowing the change of number of phonon excitations N, which in turn change the SU(3) and SO(3) content according to the reduction rules], the core is no longer inert. In our application the fermion angular momentum I is algebraically added to (subtracted from) the changing core angular momentum L, that is, the particle is "dragged" around in the symplectic core. In some sense, in contrast to the IBFM, the situation here is inverted: we have an active boson core and an inert fermion part. Physically, this does *not* correspond to the "weak-coupling limit" (as should be if N was fixed) between the core and the particle as it does in the case of IBFM (on this level of coupling). In this way, in the present approach the nuclear dynamics is completely determined by the boson degrees of freedom and the combined boson-fermion system is essentially a new rotor with slightly different bulk properties, such as moment of inertia, and so on.

IV. THE ENERGY SPECTRA OF ODD-MASS AND ODD-ODD NUCLEI

We can label the basis states according to the chain (12) as

$$|[N]_6; (\lambda, \mu); KL; I; JJ_0; T_0\rangle$$
$$\equiv |[N]_6; (N, T); KL; I; JJ_0; T_0\rangle, \quad (13)$$

where $[N]_6$, the U(6) labeling quantum number, and (λ, μ), the SU(3) quantum numbers, characterize the core excitations, K is the multiplicity index in the reduction SU(3) $\supset$ SO(3), L is the core angular momentum, I is the intrinsic spin of an odd particle (or the common spin of two fermion particles for the case of odd-odd nuclei), J, J_0 are the total (coupled boson-fermion) angular momentum and its third projection, and T, T_0 are the T spin and its third projection, respectively.

The infinite set of basis states classified according to the reduction chain (12) is schematically shown in Table I. The fourth and fifth columns show the $SO^B(3)$ content of the $SU^B(3)$ group, given by the standard Elliott reduction rules [42], while the next column gives the possible values of the common angular momentum J, obtained by coupling of the orbital momentum L with the spin I. The latter is vector coupling and hence all possible values of the total angular momentum J should be considered. For simplicity, only the maximally aligned ($J = L + I$) and maximally antialigned ($J = L - I$) states are illustrated in Table I.

The basis (13) can be considered as an angular momentum product of the orbital $|(N, T); KLM; T_0\rangle$ and spin $|IM_I\rangle$ (or for the two-particle case $|I_p, I_n; IM_I\rangle$) wave functions. Then, if the parity of the single particle is π_{sp}, the parity of the collective states of the odd-A nuclei will be $\pi = \pi_{core}\pi_{sp}$ [27]. In analogy, one can write $\pi = \pi_{core}\pi_{sp}(1)\pi_{sp}(2)$ for the case of odd-odd nuclei. Thus, the description of the positive- and/or negative-parity bands requires only the proper choice of the core bandheads, on which the corresponding single particle(s)

TABLE I. Classification scheme of basis states (13) according the decompositions given by the chain (12).

N	T	(λ, μ)	K	L	$J = L \pm I$
0	0	(0, 0)	0	0	I
2	1	(2, 0)	0	0, 2	I; $2 \pm I$
	0	(0, 1)	0	1	$1 \pm I$
	2	(4, 0)	0	0, 2, 4	I; $2 \pm I$; $4 \pm I$
4	1	(2, 1)	1	1, 2, 3	$1 \pm I$; $2 \pm I$; $3 \pm I$
	0	(0, 2)	0	0, 2	I; $2 \pm I$
	3	(6, 0)	0	0, 2, 4, 6	I; $2 \pm I$; $4 \pm I$; $6 \pm I$
	2	(4, 1)	1	1, 2, 3, 4, 5	$1 \pm I$; $2 \pm I$; $3 \pm I$; $4 \pm I$; $5 \pm I$
6	1	(2, 2)	2	2, 3, 4	$2 \pm I$; $3 \pm I$; $4 \pm I$
			0	0, 2	I; $2 \pm I$
	0	(0, 3)	0	1, 3	$1 \pm I$; $3 \pm I$
$\vdots$	$\vdots$	$\vdots$	$\vdots$	$\vdots$	$\vdots$

is (are) coupled, generating in this way the different odd-A (odd-odd) collective bands.

The Hamiltonian of the combined boson-fermion system can be written as

$$H = H_B + H_F + H_{BF}, \quad (14)$$

where the fermion degrees of freedom, coupled to the boson core, are incorporated through the terms coming from the orthosymplectic extension of the model:

$$H_F + H_{BF} = \eta I^2 + \gamma J^2 + \zeta J_0^2. \quad (15)$$

The Hamiltonian (14) is diagonal in the basis (13). Then its eigenvalues that yield the spectrum of the odd-mass and odd-odd systems are

$$E(N; T, T_0; L, I; J, J_0)$$
$$= aN + bN^2 + \alpha_3 T(T + 1) + \beta_3 L(L + 1) + \alpha_1 T_0^2$$
$$+ \eta I(I + 1) + \gamma J(J + 1) + \zeta J_0^2. \quad (16)$$

The last term is needed only for the calculation of the energies of the odd-mass neighboring nuclei.

Guided by the microscopic foundation of IBFM [43–45], where it is shown that the most important term in the boson-fermion interaction is the dynamical (quadrupole) one, we introduce in the Hamiltonian (14) an additional interaction between the core and the combined two-particle system of quadrupole type:

$$H_{int} = k Q_B \cdot Q_F, \quad (17)$$

where $Q_B = \sqrt{6} \sum_\alpha A_M^2(\alpha, \alpha)$ and $Q_F = Q_\pi + Q_\nu$ are the boson and fermion quadrupole operators, respectively. The matrix element of H_{int} between the basis states (13) can be written as

$$\langle L'\tau', I'; J|Q_B \cdot Q_F|L\tau, I; J\rangle$$
$$= (-1)^{J+L+I'} \begin{Bmatrix} L & J & I \\ I' & 2 & L' \end{Bmatrix}$$
$$\times \langle L'\gamma'||Q_B||L\gamma\rangle\langle j_\pi j_\nu I'||Q_F||j_\pi j_\nu I\rangle, \quad (18)$$

where $L' = L \mp 2$, $I' = I \pm 2$, and $\{^{L\,J\,I}_{I'\,2\,L}\}$ stands for $6j$ symbol. The labels τ and τ' denote the other quantum numbers of the basis states in chain (12). The required reduced matrix elements entering in (18) are given in Appendix B. The important point here is that the boson (L) and fermion (I) angular momenta constituting J are changed by two units in such a way as to preserve their sum always as $J' = J$. The expectation value of H_{int} will give a correction $\Delta E = \Delta E(N_0, L, I; n, j)$ to the energies (16), but will preserve the value of total (combined boson-fermion) angular momentum J, characterizing each observed state of the yrast or yrare band.

V. NUMERICAL RESULTS

In our application, the most important point is the identification of the experimentally observed states with a certain subset of basis states from (ortho)symplectic extension of the model. In general, except for the excited γ band of the even-even nucleus ^{128}Xe for which the stretched states of the first type (λ-changing) are used, the stretched states of the second type (μ-changing) are considered in all the calculations of the collective states of the neighboring odd-mass and doubly odd nuclei.

In addition to the five parameters a, b, α_3, β_3, α_1 entering in Eq. (16) which are fitted to the energies of the even-even core nucleus, the number of adjustable parameters needed for the complete description of the collective spectra of both odd-A and odd-odd nuclei is four, namely, γ, ζ, η, and k. The first two are evaluated by a fit to the experimental data [35] of the lowest negative-parity band of the corresponding odd-A neighbor, while the last two are introduced in the final step of the fitting procedure for the odd-odd nucleus, respectively. Their numerical values are $\gamma = 0.007\,38$, $\zeta = 0.009\,86$, $\eta = 0.113\,38$, and $k = 2.281\,15$. Hence, as a result of the whole fitting procedure we are able to describe simultaneously the energy spectra of the four neighboring nuclei with the same set of parameters.

The odd-A neighboring nucleus ^{127}Xe can be considered as a neutron-hole coupled to the even-even core ^{128}Xe. The low-lying positive-parity states of the GSB in the odd-A neighbor are based on positive-parity proton and positive-parity neutron configurations ($s_{\frac{1}{2}}, d_{\frac{3}{2}}, d_{\frac{5}{2}}, g_{\frac{7}{2}}$), whereas those of negative parity are based on $h_{11/2}$. Thus, we take into account only the single-particle orbit $j_1 = 11/2$. The comparison between the experimental and calculated spectra for the lowest negative-parity band in ^{127}Xe is illustrated in Fig. 3. One can see from the figure that the calculated energy levels agree well with the experimental data. The comparison between the experimental and calculated spectra (with the same set of parameters) for the lowest negative-parity structure in the odd-proton neighbor ^{129}Cs is illustrated in Fig. 4.

For the calculation of the odd-odd nuclei spectra, a second particle should be coupled to the core. In our calculations a consistent procedure is employed that includes the analysis of the even-even and odd-even neighbors of the nucleus under consideration. Thus, as a first step an odd particle was coupled to the boson core ^{128}Xe in order to obtain the spectra of the odd-mass neighbor ^{127}Xe. As a second step, we consider the addition of a second particle on a single $j_2 = 11/2$ level to the boson-fermion system. The level scheme presenting the doublet band structure in ^{128}Cs, where both the proton and neutron odd particles occupy the same single-particle level $j = j_1 = j_2 = 11/2$, is shown in Fig. 5. For comparison, the CQPCM [6] and QCM [25] results are also shown. In our model considerations, the states of the doublet bands are mapped onto the stretched SU(3) multiplets (λ_0, μ_0), $(\lambda_0, \mu_0 + 1)$, $(\lambda_0, \mu_0 + 2)$, ..., where the bandhead structures for the yrast and sidebands are determined by $(\lambda_0 = 0, \mu_0 = 11)$ (or $N_0 = 22$) and $(\lambda_0 = 8, \mu_0 = 9)$ ($N_0 = 26$), respectively. From the figure one can see that, except for the first (9^+) and last (20^+) positive states of yrast band, there is a very good agreement between the theoretical predictions and experiment up to very high angular momenta for both yrast and sidebands, which reveals the applicability of the used dynamical symmetry of the model.

The similar level scheme of ^{128}Cs indicates that this nucleus can be interpreted as having a chiral structure. However, the energy splitting of these bands connected with the extent of violation of chiral symmetry [19] is about 200 keV. Although the partner bands are not degenerate as should be in the ideal chiral situation, this is the first indication that the partner bands in ^{128}Cs might have properties closer to the expected features of chiral bands. To investigate the structure of the doublet bands in a certain nucleus, it is crucial to determine the $B(E2)$ and $B(M1)$ values, which are very important for establishing the nature of these bands. So, in the next section we consider the $E2$ and $M1$ transitions in the framework of the IVBFM.
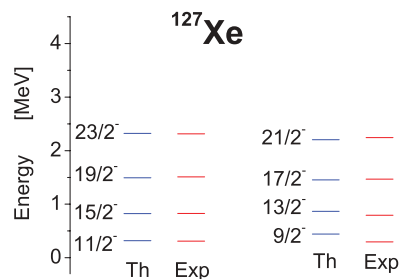

FIG. 3. (Color online) Comparison of the theoretical and experimental energies for the lowest negative-parity states built on the $h_{11/2}$ configuration in ^{127}Xe.
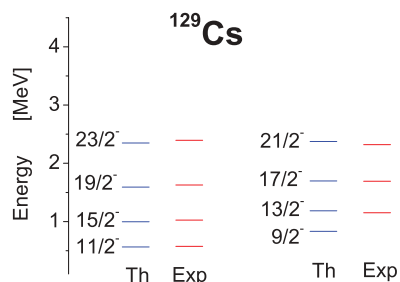

FIG. 4. (Color online) Comparison of the theoretical and experimental energies for the lowest negative-parity states built on $h_{11/2}$ configuration in ^{129}Cs.
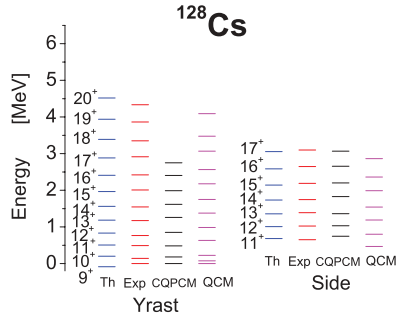
FIG. 5. (Color online) Comparison of the theoretical and experimental energies for the yrast and sidebands of ^{128}Cs. The theoretical predictions of the CQPCM are shown as well. The used values of the model parameters are as follows: $a = 0.089\,09$, $b = -0.004\,59$, $\alpha_3 = 0.024\,71$, $\beta_3 = 0.031\,23$, $\alpha_1 = -0.019\,89$, $\gamma = 0.007\,38$, $\zeta = 0.009\,86$, $\eta = 0.113\,38$, and $k = 2.281\,15$.

VI. ELECTROMAGNETIC TRANSITIONS

In this section we calculate the $B(E2)$ and $B(M1)$ transition probabilities between the states of the partner bands and compare them with their absolute values measured in the experiment [29].

The $E2$ transition operator between the states of the considered band is defined as [28,46]

$$T^{E2} = e\Big[A^{[1-1]_6\quad 20}_{(1,1)_3[0]_2\quad 00} + \theta\Big([F \times F]^{[4]_6\quad 20}_{(0,2)[0]_2\quad 00}$$
$$+ [G \times G]^{[-4]_6\quad 20}_{(2,0)[0]_2\quad 00}\Big)\Big], \tag{19}$$

where the symbols $[\ ]_6$, $(,\ )_3$, and $[\ ]_2$ denote the corresponding U(6), SU(3), and U(2) irreducible representations, respectively. In (19) the notation $[A \times B]^{[N]_6\quad LM}_{(\lambda,\mu)[2T]_2\ TT_0}$ for the tensor coupling of two tensors A and B to the respective final representations is also used. The first part of (19) is an SU(3) generator and actually changes only the angular momentum with $\Delta L = 2$, whereas the second term changes both the number of bosons by $\Delta N = 4$ and the angular momentum by $\Delta L = 2$. In (19) e is the effective boson charge fitted together with θ to the experimental data on the transitions.

The theoretical predictions for the $B(E2)$ values for ^{128}Cs are compared with the experimental data [29] and the CQPCM [29] and QCM [25] results in Fig. 6. The values used for the two model parameters are $e = 0.86$ and $\theta = -0.0024$. In our approach, the odd-spin and even-spin members of the yrast or sideband form two $\Delta J = 2$ $E2$ bands with the sequences $J, J + 2, J + 4, \ldots$ and $J + 1, J + 3, \ldots$ which are built on two different bandhead configurations having an intrinsic spin I (=8) and $I - 2$ (=6), respectively. The different two-particle configurations I are caused by the relative motion of the two angular momenta of the proton and the neutron, which open and close sequentially ("scissorslike" motion), thus changing I by $\Delta I = 2$ in the following way: $I \rightarrow I - 2 \rightarrow I$. From the figure one can see the good overall reproduction of the experimental values. The $B(E2)$ values in the yrast band are 20%–60% larger than in the sideband.

In Fig. 7 we show the behavior of the quadrupole moments $Q(J)$ as a function of the angular momentum J for the yrast and sidebands in ^{128}Cs.
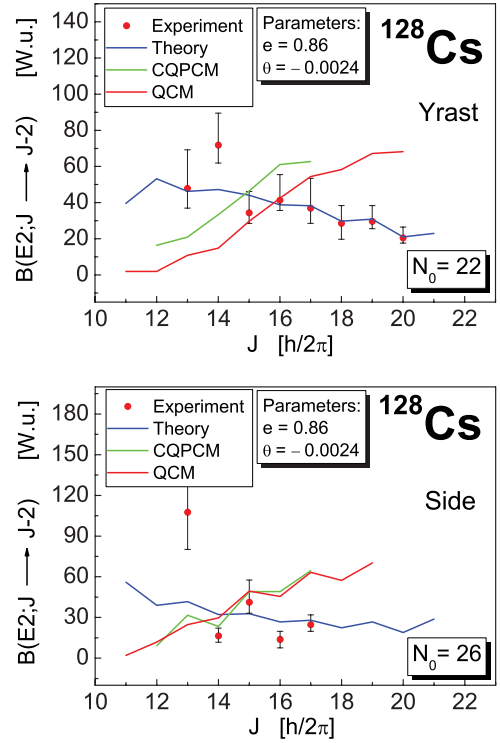

FIG. 6. (Color online) Comparison of the theoretical and experimental values for the $B(E2)$ transition probabilities between the states of yrast and sidebands for ^{128}Cs. The theoretical predictions of the CQPCM and QCM are shown as well. The values of the model parameters are $e = 0.86$ and $\theta = -0.0024$.

The structure of the $M1$ transition operator between the states of the yrast and yrare bands is defined as [28]

$$T^{M1}\ {}^{(1)}_M = \sqrt{\frac{3}{4\pi}}\Big[g\,J^{(1)}_M + g_{FG}\Big(F^{[2]_6\quad 1M}_{(0,1)[0]_2\quad 00}$$
$$+ G^{[-2]_6\quad 1M}_{(1,0)[0]_2\quad 00}\Big)\Big]. \tag{20}$$

$J^{(1)}_M$ is the total boson-fermion angular momentum, that is, $J^{(1)}_M = L^1_M + I^{(1)}_M$, where $L^1_M = -\sqrt{2}\sum_\alpha A^1_M(\alpha, \alpha)$ and
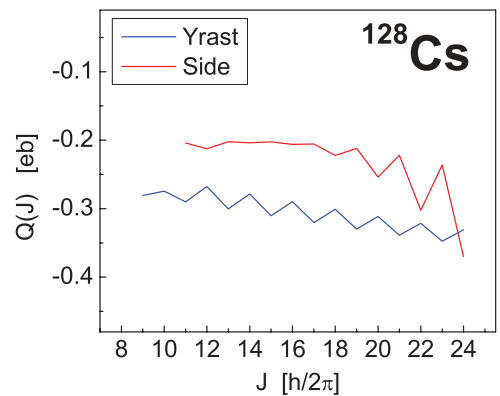

FIG. 7. (Color online) Theoretical values of the quadrupole moments $Q(J)$ as a function of the angular momentum J for both yrast and sidebands in ^{128}Cs.
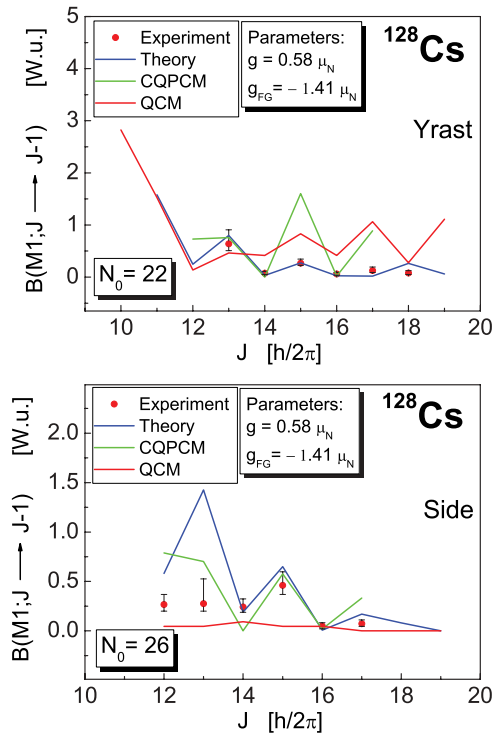
FIG. 8. (Color online) Comparison of the theoretical and experimental values for the $B(M1)$ transition probabilities between the states of yrast and sidebands for ^{128}Cs. The theoretical predictions of the CQPCM and QCM are shown as well. The values of the model parameters are $g = 0.58\mu_N$ and $g_{FG} = -1.41\mu_N$.

$I_M^{(1)} = [a_j^\dagger a_j]_M^{(1)}$. The obtained values of the effective g factors are $g = 0.58\mu_N$ and $g_{FG} = -1.41\mu_N$.

The theoretical predictions for the intraband $B(M1)$ values for the partner bands in ^{128}Cs are compared with the experimental data and the CQPCM [29] and QCM [25] results in Fig. 8. The spin dependence of the reduced $M1$ transition probabilities inside each of the bands shows characteristic staggering and, except for the state $J = 13$ of the sideband, is reproduced reasonably well. The $B(M1)$ values between the states of both the yrast and sidebands (less pronounced) for the transitions from the odd-spin states to the even-spin states are larger than for the transitions from even-spin to odd-spin states. The strong $M1$ transitions connect the odd-spin states $(J + 1)$ built on the bandhead with the intrinsic spin I to the even-spin states (J) which possess a bandhead configuration with $I - 2$. The difference of the two-particle structures for the two sequences with odd and even values of J, caused by the scissorslike motion of the proton and the neutron, is the reason for the staggering in the $B(M1)$ behavior, which has larger amplitude in the sideband than in the yrast band. The different amplitude of the $B(M1)$ staggering in the two bands is a result of the different structure of the stretched states used, which for the yrast and sidebands are determined by the SU(3) multiplets $(0, \mu)$ and $(8, \mu)$, respectively. The $B(M1)$ values in the yrast band are 5%–30% larger than in the sideband. From Fig. 8 one can see that the $B(M1)$ curves of the QCM and IVBFM for the yrast band show very similar behavior. At this point we want to point out that the interpretation of the structure of

doublet bands in the present work is very similar to that given in Refs. [23–25], especially the assignment of the states to the two $\Delta J = 2$ $E2$ bands comprising the doublet bands and the corresponding quadrupole transitions. Concerning the $M1$ transitions, the structure of the $M1$ sequences in the PTSM and QCM is rather different (especially at the "bottom" of the bands) from that presented here.

In the picture of the chiral structure, the total angular momentum is tilted with respect to the planes defined by the three principal axes. This situation is realized when the angular momenta of the valence proton, the valence neutron, and the triaxial core tend to align with the short, long, and intermediate axes, respectively. It indicates that the three considered angular momenta tend to be perpendicular to each other. The deformation in the partner bands is the same, as well as the structure of the corresponding states in the partner bands.

Since the IVBFM is an algebraic model based on a set of algebraic assumptions, the interpretation of its results in terms of space orientation of the three angular momenta is not evident. First, as we are interested in the dynamical symmetry $SO^F(2\Omega) \supset Sp(\Omega) \supset SU^F(2)$, we approach the problem by considering the simplest physical picture in which two particles with the same intrinsic j are coupled to an even-even nucleus. This simplification that occurs when the fermion and boson degrees of freedom are coupled on the level of the angular momenta (and hence the neutron and proton states are not distinguished) weakens the full fermion contribution to nuclear wave functions and dynamics. If the two particles were treated as different, a new fermion dynamical chain should be considered in which both the spin and isospin degrees of freedom are involved in the fermion sector, which would introduce additional parameters in the energy formula and make the identification of the bands parameter dependent. Nevertheless, the result that the states of the partner bands are built on proton-neutron configurations with angular momentum much smaller than the maximal alignment suggests that the condition of their almost perpendicular orientation can be achieved. However, this chiral-like picture is disturbed by the scissorslike motion of the two angular momenta of the neutron and the proton in the two-particle system.

In the boson sector the adopted algebraic concept of "yrast" states makes the geometrical interpretation less transparent. In our approach the states of the yrast band are built on the ground-state bandlike SU(3) multiplets $(0, \mu)$ of the even-even core, while those of the sideband are built on the SU(3) multiplets $(8, \mu)$, which could suggest similar [both sets of SU(3) multiplets are stretched states of the second type], but not equal, collective behavior of the two bands. This is reflected in the $E2$ transitions, possibly pointing to different deformations in partner bands. The calculated quadrupole moments, which are around 50% smaller in the side than in the yrast band, strengthen the conclusion that in the IVBFM the two bands are built on different deformations.

The results of our calculations show that the structure of ^{128}Cs and its even-even and odd-even neighbors ^{128}Xe, ^{127}Xe, and ^{129}Cs can be described in a consistent approach based

on the dynamical supersymmetry group OSp($2\Omega/12$, R). This suggests that the appearance of doublet bands in certain odd-odd nuclei could be a consequence of a larger symmetry (supersymmetry) than those that arise in geometrical models. Over the last few decades different supersymmetric extensions of the IBM [47] with its three boson dynamical symmetries for the core were exploited, with Hamiltonians that exhibit dynamical supersymmetries based on the compact supergroups of the type U(n/m). In this respect, the comparison of the theoretical predictions of both compact and noncompact dynamical supersymmetries is of particular interest. In the case of ^{128}Cs, our calculations suggest that the symmetry is partially broken by the additional interaction between the core and the two-fermion system, but is still approximately realized.

VII. CONCLUSIONS

In the present paper, the yrast and yrare states with the $\pi h_{11/2} \otimes \nu h_{11/2}$ configuration in ^{128}Cs were investigated in terms of the IVBFM. This allows for the proper reproduction of the energies of these states up to very high angular momenta in both bands. The even-even nucleus ^{128}Xe is used as a core on which the collective excitations of the neighboring odd-mass and odd-odd nuclei are built. Thus, the spectra of odd-mass and odd-odd nuclei arise as a result of the consequent and self-consistent coupling of the fermion degrees of freedom to the boson core. Therefore, according to our approach a purely collective nature is assigned to the states of the partner bands.

The $B(E2)$ and $B(M1)$ transition probabilities between the states of the yrast and sidebands are calculated and compared with the experimental data. A very good overall agreement of the theoretical predictions with experiment, including the staggering patterns, is obtained. The contribution of the symplectic term entering into the corresponding transition operators turns out to be crucial for the accurate reproduction of the experimental behavior. The observed staggering in the $B(M1)$ [and $B(E2)$] values is reproduced within our theoretical framework by introducing a quadrupole interaction between the core and two-particle system, which produces such a staggering effect in the transition strengths.

The consistent description of the structure of ^{128}Cs and its even-even and odd-even neighbors ^{128}Xe, ^{127}Xe, and ^{129}Cs suggests that the appearance of partner bands in certain odd-odd nuclei could be a consequence of a larger symmetry (supersymmetry) than those that arise in geometrical models, pointing to the possible realization of noncompact dynamical supersymmetries in heavy nuclei.

ACKNOWLEDGMENTS

APPENDIX A: TWO-PARTICLE STATE OF NEUTRON AND PROTON

We consider a two-particle system of one neutron and one proton particle in the same orbital j, where j symbolically represents the quantum numbers (n, l, j). The wave function characterized by the total spin I and its projection M_I is written as

$$|jj; IM_I\rangle = \sum_{M_1 M_2} (jM_1 jM_2 | IM) |jM_1\rangle_p |jM_2\rangle_n$$
$$= [|j\rangle_p \otimes |j\rangle_n]^I_{M_I}, \tag{A1}$$

where $|jM\rangle_\tau$ ($\tau = p$ or n) denotes a single-particle state and (j, m) represents a set of quantum numbers necessary to specify the state (n, l, j, m). We adopt $j = 11/2$, $l = j - 1/2 = 5$, and $n = 0$ to represent the intruder orbital $0h_{11/2}$ in the 50–82 major shell.

APPENDIX B: REDUCED MATRIX ELEMENTS

The reduced matrix element $\langle L'\tau' || Q_B || L\tau \rangle$ of the boson quadrupole operator $Q_B = A^{[1-1]_6 \quad 2M}_{(1,1)_3[0]_2 \quad 00}$ is given by [46]

$$\langle [N], (\lambda', \mu'); K'L'; T'T'_0 | \left| A^{[1,-1]_6 \quad lm}_{(1,1)[0]_2 \quad 00} \right| | [N], (\lambda, \mu); KL; TT_0 \rangle$$
$$= \delta_{TT'} \delta_{T_0 T'_0} \delta_{\lambda\lambda'} \delta_{\mu\mu'} \sum_{\rho=1,2} C^{(\lambda,\mu) \quad (1,1) \quad \rho(\lambda',\mu')}_{K(L) \quad k(l) \quad K'(L')}$$
$$\times \langle [N], (\lambda', \mu') | \left| A^{[1,-1]_6}_{(1,1)[0]_2} \right| | [N], (\lambda, \mu) \rangle, \tag{B1}$$

where $C^{(\lambda,\mu) \quad [\lambda]_3 \quad (\lambda',\mu')}_{KL \quad k(l)_3 \quad K'L'}$ is the reduced SU(3) Clebsch-Gordan coefficient and the reduced triple-barred matrix element for $\rho = 1$ is

$$\langle [N], (\lambda, \mu) | \left| A^{[1-1]_6}_{(1,1)_3[0]_2} \right| | [N], (\lambda, \mu) \rangle_1 = \begin{cases} g_{\lambda\mu}, & \mu = 0, \\ -g_{\lambda\mu}, & \mu \neq 0, \end{cases} \tag{B2}$$

where

$$g_{\lambda\mu} = 2\left(\frac{\lambda^2 + \mu^2 + \lambda\mu + 3\lambda + 3\mu}{3}\right)^{1/2}. \tag{B3}$$

For $\rho = 2$ we have

$$\langle [N], (\lambda, \mu) | \left| A^{[1-1]_6}_{[210]_3[0]_2} \right| | [N], (\lambda, \mu) \rangle_2 = 0. \tag{B4}$$

The reduced matrix element of a quadrupole operator for the two-particle state is written as

$$\langle jjI' || Q_\tau || jjI \rangle = (-1)^{2j+I} \sqrt{(2I+1)(2I'+1)}$$
$$\times \begin{Bmatrix} I' & 2 & I \\ j & j & j \end{Bmatrix} \langle j || Q_\tau || j \rangle, \tag{B5}$$

where the reduced matrix element $\langle j || Q_\tau || j \rangle$ is given by

$$\langle j || Q_\tau || j \rangle = \langle nl | r^2 | nl \rangle \langle j || Y^2 || j \rangle, \tag{B6}$$

where $\tau = \pi, \nu$ and

$$\langle nl | r^2 | nl \rangle = (2n + l + 3/2) = j + 1, \tag{B7}$$

$$\langle j || Y^2 || j \rangle = (-1)^{j+1/2} \sqrt{\frac{5(2j+1)}{4\pi}} \begin{pmatrix} j & 2 & j \\ \frac{1}{2} & 0 & -\frac{1}{2} \end{pmatrix}. \tag{B8}$$

Here, again we take $l = j - 1/2$ and $n = 0$.

[1] K. Starosta *et al.*, Phys. Rev. Lett. **86**, 971 (2001).

[2] A. A. Hecht *et al.*, Phys. Rev. C **63**, 051302(R) (2001).

[3] T. Koike, K. Starosta, C. J. Chiara, D. B. Fossan, and D. R. LaFosse, Phys. Rev. C **63**, 061304(R) (2001).

[4] D. J. Hartley *et al.*, Phys. Rev. C **64**, 031304(R) (2001).

[5] R. A. Bark *et al.*, Nucl. Phys. A **691**, 577 (2001).

[6] T. Koike, K. Starosta, C. J. Chiara, D. B. Fossan, and D. R. LaFosse, Phys. Rev. C **67**, 044319 (2003).

[7] K. Starosta *et al.*, Phys. Rev. C **65**, 044328 (2002).

[8] G. Rainovski *et al.*, Phys. Rev. C **68**, 024318 (2003).

[9] S. Frauendorf and J. Meng, Nucl. Phys. A **617**, 131 (1997).

[10] V. I. Dimitrov, S. Frauendorf, and F. Dònau, Phys. Rev. Lett. **84**, 5732 (2000).

[11] A. J. Simons *et al.*, J. Phys. G **31**, 541 (2005).

[12] T. Koike, K. Starosta, and I. Hamamoto, Phys. Rev. Lett. **93**, 172502 (2004).

[13] I. Ragnarsson and P. Semmes, Hyperfine Interact. **43**, 423 (1988).

[14] Ch. Droste *et al.*, Eur. Phys. J. A **42**, 79 (2009).

[15] S. Brant, D. Vretenar, and A. Ventura, Phys. Rev. C **69**, 017304 (2004).

[16] E. Grodner, J. Srebrny, Ch. Droste, T. Morek, A. Pasternak, and J. Kownacki, Int. J. Mod. Phys. E **13**, 243 (2004).

[17] D. Tonev *et al.*, Phys. Rev. Lett. **96**, 052501 (2006).

[18] C. M. Petrache, G. B. Hagemann, I. Hamamoto, and K. Starosta, Phys. Rev. Lett. **96**, 112502 (2006).

[19] K. Starosta, T. Koike, C. J. Chiara, D. B. Fossan, and D. R. Lafosse, Nucl. Phys. A **682**, 375c (2001).

[20] C. Vaman, D. B. Fossan, T. Koike, K. Starosta, I. Y. Lee, and A. O. Macchiavelli, Phys. Rev. Lett. **92**, 032501 (2004).

[21] S. Mukhopadhyay *et al.*, Phys. Rev. Lett. **99**, 172501 (2007).

[22] B. Qi, S. Q. Zhang, S. Y. Wang, J. M. Yao, and J. Meng, Phys. Rev. C **79**, 041302(R) (2009).

[23] K. Higashiyama and N. Yoshinaga, Prog. Theor. Phys. **113**, 1139 (2005); K. Higashiyama, N. Yoshinaga, and K. Tanabe, Phys. Rev. C **72**, 024315 (2005); N. Yoshinaga and K. Higashiyama, J. Phys. G **31**, S1455 (2005).

[24] N. Yoshinaga and K. Higashiyama, Eur. Phys. J. A **30**, 343 (2006); **31**, 395 (2007).

[25] K. Higashiyama and N. Yoshinaga, Eur. Phys. J. A **33**, 355 (2007).

[26] V. Paar, in *Capture Gamma-Ray Spectroscopy and Related Topics*, edited by S. Raman, AIP. Conf. Proc. No. 125 (AIP, New York, 1985), p. 70; S. Brant, V. Paar, and D. Vretenar, Z. Phys. A **319**, 355 (1984); V. Paar, D. K. Sunko, and D. Vretenar, *ibid.* **327**, 291 (1987); S. Brant and V. Paar, *ibid.* **329**, 151 (1988).

[27] H. G. Ganev, J. Phys. G **35**, 125101 (2008).

[28] H. G. Ganev, A. I. Georgieva, S. Brant, and A. Ventura, Phys. Rev. C **79**, 044322 (2009); in *Proceedings of 28th International Workshop on Nuclear Theory, Rila Mountains, Bulgaria, 2009*, edited by S. Dimitrova (BM Trade, Sofia, Bulgaria, 2009), p. 177.

[29] E. Grodner *et al.*, Phys. Rev. Lett. **97**, 172501 (2006).

[30] X. Li *et al.*, Chin. Phys. Lett. **19**, 1779 (2002); S. Wang, Y. Liu, T. Komatsubara, Y. Ma, and Y. Zhang, Phys. Rev. C **74**, 017302 (2006); S. Y. Wang, S. Q. Zhang, B. Qi, and J. Meng, *ibid.* **75**, 024309 (2007).

[31] U. Yong-Nam *et al.*, J. Phys. G **31**, B1 (2005).

[32] H. Ganev, V. P. Garistov, and A. I. Georgieva, Phys. Rev. C **69**, 014305 (2004).

[33] D. J. Rowe, Rep. Prog. Phys. **48**, 1419 (1985).

[34] H. G. Ganev, V. P. Garistov, A. I. Georgieva, and J. P. Draayer, Phys. Rev. C **70**, 054317 (2004).

[35] Evaluated Nuclear Structure Data File (ENSDF) [http://ie.lbl. gov/databases/ensdfserve.html].

[36] L. Wilets and M. Jean, Phys. Rev. **102**, 788 (1956).

[37] D. Bonatsos *et al.*, Rom. J. Phys. **52**, 779 (2007).

[38] R. F. Casten, *Nuclear Structure from a Simple Perspective* (Oxford University Press, Oxford (1990).

[39] D. Bonatsos, D. Lenis, N. Pietralla, and P. A. Terziev, Phys. Rev. C **74**, 044306 (2006).

[40] Nuclear Levels and Gammas Search [http://www.nndc. bnl.gov/].

[41] B. G. Wybourne, *Classical Groups for Physicists* (Wiley, New York, 1974).

[42] J. P. Elliott, Proc. R. Soc. London Ser. A **245**, 562 (1958).

[43] I. Talmi, in *Interacting Bose-Fermi Systems in Nuclei*, edited by F. Iachello (Plenum, New York, 1981), p. 329.

[44] O. Scholten and A. E. L. Dieperink, in *Interacting Bose-Fermi Systems in Nuclei* (Ref. [43]), p. 343.

[45] O. Scholten, Prog. Part. Nucl. Phys. **14**, 189 (1985).

[46] H. G. Ganev and A. I. Georgieva, Phys. Rev. C **76**, 054322 (2007).

[47] F. Iachello, Phys. Rev. Lett. **44**, 772 (1980); A. B. Balantekin, I. Bars, R. Bijker, and F. Iachello, Phys. Rev. C **27**, 1761 (1983); P. Van Isacker, J. Jolie, K. Heyde, and A. Frank, Phys. Rev. Lett. **54**, 653 (1985); A. Metz *et al.*, *ibid.* **83**, 1542 (1999); J. Barea, R. Bijker, A. Frank, and G. Loyola, Phys. Rev. C **64**, 064313 (2001); J. Barea, R. Bijker, and A. Frank, J. Phys. A **37**, 10251 (2004); Phys. Rev. Lett. **94**, 152501 (2005).